Autonomous DC-Link Voltage Restoration for Grid-Connected Power Converters Providing Virtual Inertia

Ke Guo
Energy Research Institute @ NTU, ERI@N, Interdisciplinary Graduate School
Nanyang Technological University
Singapore
ke004@e.ntu.edu.sg

Jingyang Fang
School of Electrical and Electronic Engineering
Nanyang Technological University
Singapore
jfang006@e.ntu.edu.sg

Yi Tang
School of Electrical and Electronic Engineering
Nanyang Technological University
Singapore
yitang@ntu.edu.sg

***Abstract*—Renewable energy sources have been increasingly adopted to reduce greenhouse emissions. However, they are normally interfaced with power grids through grid-connected power converters without any inertia contribution. This will lead to the decreased power system inertia. As a solution, the method of inertia emulation by power converters has been reported to handle this problem. However, the DC-link capacitors of power converters cannot restore their voltages after injecting the power required by inertia emulation. Thus, if the load change causes another DC-link voltage drop, the undesirable overmodulation may appear. Moreover, power converters cannot provide multiple inertia support during cascading frequency events without the DC-link voltage recovery. To address the above concerns, this paper proposes an autonomous DC-link voltage restoration method that allows the restoration of DC-link voltages after individual frequency events. Simulation and experimental results verify the feasibility of the proposed method.**

Keywords—capacitor, filter, frequency control, power converter, virtual inertia

I. Introduction

The penetration level of renewable energies has been increasing in recent years. However, unlike synchronous generators, renewable generators such as wind turbines and photovoltaic (PV) arrays are interfaced with power girds through power converters without the rotational inertia. This is because renewable generators normally operate to optimize the energy yield and do not store the kinetic energy [1, 2]. Therefore, as synchronous generators being replaced by renewable generators, the power system inertia decreases [3]. The ever-decreasing inertia translates into high rate-of-change-of-frequency (RoCoF) levels and low frequency nadir, which may cause tripping of generators and even grid collapses [4].

As increasing inertia is very desirable, the concept of virtual inertia has been proposed and used to enhance the power system inertia. In [5], the pitch angle of the wind turbine is controlled in such a way that the turbine operates below the maximum power point and part of the wind energy is reserved for inertia emulation. However, this approach necessitates the curtailment of wind power and thus incurring a nontrivial opportunity cost. In [6], the rotor speed of the wind turbine is tightly regulated to exploit the kinetic energy stored in the rotor for inertia emulation. However, rotor speed variations increase the mechanical stress on the wind turbine, and the recovery of the rotor speed may cause a second frequency drop, which may deteriorate the power system stability.

Recently, energy storage systems (ESSs) are showing great promise for inertia emulation. As an example, a hybrid system consisting of an ESS and a wind generator has been proposed to provide the virtual inertia for minimizing frequency deviations [7]. In [8], a flywheel storage system, together with a wind power generation system, has been employed for inertia emulation, and a central controller is used to coordinate these two systems. Although having great potentials, ESSs necessitate high capital and operating costs, which may increase the financial burden on power systems [9].

Another potential inertia supplier is the grid-connected converter (GCC). In this case, the energy stored in the DC-link capacitors of GCCs can be used to emulate inertia during frequency events. Along this research direction, the concept of distributed virtual inertia generated by GCCs has been proposed with its effectiveness verified in [10]. This method allows no hardware change, and hence it is economically attractive. Nevertheless, due to the proportional relationship between the DC-link voltage and the grid frequency, the DC-link voltage cannot restore its nominal value after releasing the power required by inertia emulation as long as the grid frequency deviation exists. Furthermore, the low DC-link voltage may lead to the overmodulation of GCCs when another DC-link voltage drop is caused by sudden load changes. Moreover, the GCCs cannot provide multiple inertia support in the face of cascading frequency events.

In view of these drawbacks, the modified virtual inertia control is proposed and utilized in this paper to restore the DC-link voltage after inertia support. It is featured by a high-pass filter (HPF), which is cascaded with the conventional virtual inertia control block to extract the high-frequency components of the grid frequency for inertia emulation. With the proposed HPF, the inertia emulation is only activated during frequency events, and the DC-link voltage can be restored after individual frequency events. Finally, simulation and experimental results verify the effectiveness of the proposed method.

II. Conventional Virtual Inertia Control

A typical power system consisting of synchronous generators (SGs), frequency dependent loads, e.g. induction motors and frequency independent loads is shown in Fig. 1, where P_m denotes the input mechanical power of SGs. P_e

signifies the output electrical power of SGs, and it can be further expressed as (P_L + P_D) if the power converters are disabled. P_L represents the power absorbed by the frequency independent loads. $P_D = D\Delta f$ denotes the power consumed by the frequency dependent loads, D refers to the damping factor. P_{GCC} refers to the power absorption of GCCs, and it is equal to the power consumed by loads minus the power generated from renewable generators interfaced by GCCs. The dynamic behavior of the power system can be described by the following swing equation [11]:

$$P_{m\_pu} - P_{e\_pu} = 2H\frac{d\Delta f_{pu}}{dt} \tag{1}$$

where H signifies the inertia constant and Δf_{pu} represents the per unit change of the grid frequency. As mentioned, great efforts have been attached to enhancing the power system inertia, which is essentially increasing the value of H.

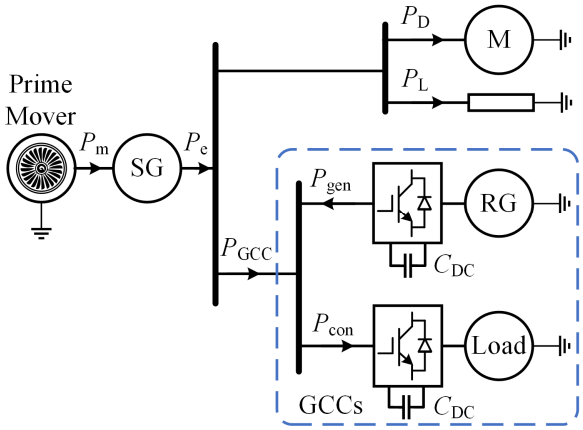

Fig. 1. Simplified model of a typical power system.

The virtual inertia generated by GCCs is proven to have a great potential for inertia improvement and already demonstrated its effectiveness in [10]. For illustration, the schematic of the GCC equipped with the virtual inertia control is shown in Fig. 2, where the DC-link capacitor of the GCC serves as a potential inertia supplier. The three-phase grid voltages are measured and then synchronized by a phase-locked-loop (PLL), which provides the phase-angle information for current regulation and grid synchronization in the synchronous dq-frame. The voltage of the DC-link capacitor v_{dc} can be controlled to its reference value v_{dc_ref} by changing the d-axis reference current i_{d_ref}. A virtual inertia control block allowing generating the virtual inertia has been introduced. It directly links the grid frequency and the DC-link voltage so that the DC-link capacitor can absorb or release the energy required by inertia emulation when the grid frequency deviates from its nominal value. Taking the effect of virtual inertia into consideration, the swing equation expressed in (1) is modified as

$$P_{m\_pu} - P_{L\_pu} - D\Delta f_{pu} - P_{GCC\_pu} = 2H\frac{d\Delta f_{pu}}{dt} \tag{2}$$

where the subscript $_{pu}$ denotes the per unit notation. Similar to H, the inertia constant of the DC-link capacitor H_c is defined as

$$H_c = \frac{C_{dc}v_{dc\_ref}^{\ 2}}{2VA_{rated}} \tag{3}$$

where v_{dc_ref} represents the rated DC-link voltage and VA_{rated} is the rated power of the GCC.

According to [10], the virtual inertia control was designed to be a proportional controller relating the DC-link voltage and the grid frequency through a gain K_{fv}, expressed as

$$K_{fv} = \frac{\Delta v_{dc\_max}}{\Delta f_{max}} \tag{4}$$

where Δv_{dc_max} and Δf_{max} are the maximum DC-link voltage change and the maximum grid frequency change, respectively. Through this method, the energy stored in the DC-link capacitor can be exploited to emulate the inertia, and the corresponding equivalent inertia constant or virtual inertia can be derived as

$$H_{vi} = \frac{C_{dc}v_{dc\_ref}^{\ 2}}{2VA_{rated}} \cdot \frac{\Delta v_{dc\_max}}{\Delta f_{max}} \tag{5}$$

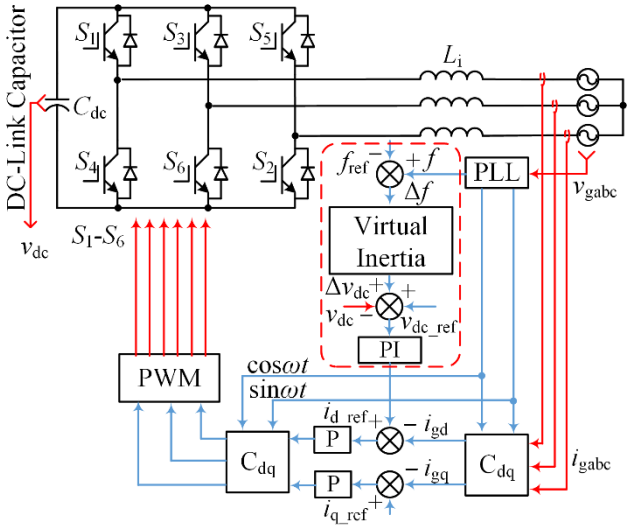

Fig. 2. Schematic of the GCC equipped with the virtual inertia control.

Although the virtual inertia control reported in [10] is promising in terms of inertia enhancement, the DC-link voltage and the grid frequency are proportionally related, and therefore the DC-link voltage cannot restore its nominal value after frequency events. Thus, once a sudden load change of the power converter causes another DC-link voltage drop, the over-modulation of the GCC may occur due to the low DC-link voltage. Besides, without the DC-link voltage recovery, the GCC cannot provide multiple inertia support for cascading frequency events. Therefore, it would be very desirable if the DC-link voltage could be recovered to its nominal value automatically.

III. Proposed Virtual Inertia Control with DC-Link Voltage Restoration

In order to automatically recover the DC-link voltage, a HPF is introduced and cascaded with the proportional controller K_{fv}. The HPF extracts only the high-frequency components of the grid frequency for inertia emulation. As a result, when the grid frequency reaches its quasi-steady-state after frequency events, the inertia emulation function of GCCs will be disabled, and the DC-link voltage will begin to restore. Under this condition, the DC-link capacitor can

restore its nominal voltage and then prepare itself for another frequency event. For demonstration, the block diagram of the frequency regulation architecture including the proposed DC-link voltage restoration block is detailed in Fig. 3, where T_G, F_{HP}, T_{RH}, T_{CH}, and R are the parameters of SGs [3].

Special attention should be paid to the HPF, as shown in Fig. 3. Its transfer function can be expressed as

$$G_{h\_pass}(s) = \frac{s}{s + 2\pi f_{cut}} \tag{6}$$

where f_{cut} denotes the cut-off frequency of the HPF. f_{cut} is essential for the DC-link voltage restoration. It can influence the effectiveness of inertia support and the DC-link voltage restoration time.

The critical part of the proposed method is the design of the cut-off frequency f_{cut}. The cut-off frequency f_{cut} has a great influence on the DC-link voltage restoration time t_{res} (time for reaching 99% nominal DC-link voltage) and the virtual inertia support accuracy of the GCC. With a large cut-off frequency, the high-frequency components of the grid frequency deviation Δf going through the HPF will decrease, and thus t_{res} will be small. However, the grid frequency deviation after the HPF will be less accurate. Due to the proportional controller K_{fv} inside the virtual inertia block, as shown in Fig. 3, the inertial power P_{GCC} exported from the GCC will be inaccurate as well, and thus leading to the insufficient virtual inertia support of the GCC during frequency events. Alternatively, if a small cut-off frequency f_{cut} is adopted, more high-frequency components of the grid frequency deviation Δf will pass through the HPF. As a result, a better virtual inertia support of the GCC can be expected. Nevertheless, a longer time t_{res} will be required for the DC-link capacitor to restore its voltage. Thus, the cut-off frequency f_{cut} should be designed considering two factors, i.e. the DC-link voltage restoration time t_{res} as well as the accuracy of virtual inertia support.

The DC-link voltage restoration time t_{res} should be small enough to allow multiple frequency support. It is noted that there are three frequency control layers. The primary frequency control aims to arrest the fast frequency decline [3]. Normally, its response time ranges from 10 to 60 seconds [12]. As the inertia responses of SGs and GCCs belong to the primary frequency control, the DC-link voltage restoration should be finished within the response time range of the primary frequency control. In [13], the restoration time of the rotor speed is designed to be 30 seconds. Following this design, the DC-link voltage restoration time t_{res} is designed to be 10-30 seconds in this paper.

Considering the accuracy of virtual inertia support, the negative effect of the HPF should be minimized so that the frequency drop will not be excessive. To quantify the effect of the HPF, an performance index σ is introduced, expressed as

$$\sigma = \frac{\Delta f_{vr} - \Delta f_{bm}}{\Delta f_{bm}} \times 100\% \tag{7}$$

in which Δf_{bm} signifies the maximum frequency deviation during the frequency event with the conventional virtual inertia control. Δf_{vr} denotes the maximum frequency deviation during the frequency event in the case of the proposed virtual inertia control. To limit the adverse effect of the HPF, σ should be less than 10%. The DC-link voltage restoration time t_{res} and the index σ as a function of the cut-off frequency f_{cut} are shown in Fig. 4, where the system parameters are listed in Table. I.

From Fig. 4, it can be noted that to satisfy both the requirements of the DC-link voltage restoration time t_{res} and the index σ, the range of the cut-off frequency f_{cut} is 0.007 to 0.013 Hz, as indicated by the overlapped area in Fig. 4.

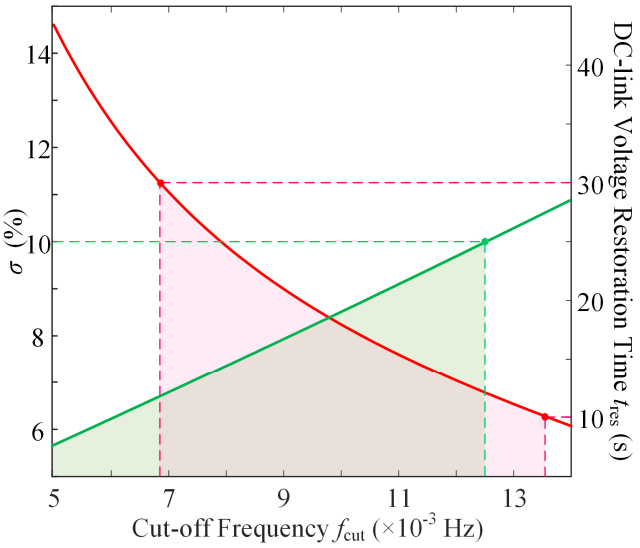

Fig. 4. Relationship between the cut-off frequency f_{cut} and the DC-link voltage restoration time t_{res} as well as the index σ.

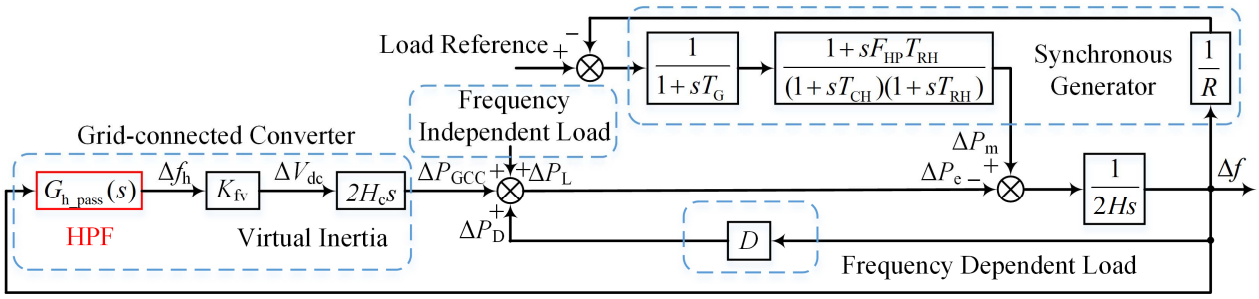

Fig. 3. Block diagram of the frequency regulation architecture including the proposed DC-link voltage recovery block.

TABLE I. SYSTEM PARAMETER VALUES

Symbol	Description	Value	Symbol	Description	Value
T_G	Speed governor coefficient	0.1 s	K_{fv}	Proportional gain	22.5
T_{CH}	Time constant of main inlet volumes	0.2 s	V_{dc}	Rated DC-link voltage	400 V
T_{RH}	Time constant of reheater	7.0 s	ΔV_{dc_max}	Maximum DC-link voltage deviation	36 V
F_{HP}	Turbine HP coefficient	0.3 s	C_{dc}	DC-link capacitance	2.82 mF
R	Droop coefficient	0.05	Δf_{max}	Maximum frequency deviation	0.2 Hz
H	Inertia coefficient of SG	5.0 s	VA_{rated}	Power rating	1000 kVA
D	Damping coefficient	1.0			

IV. SIMULATION AND EXPERIMENTAL RESULTS

A. Simulation results

The effectiveness of the proposed virtual inertia control with the DC-link voltage restoration has been verified through simulations under the Matlab/Simulink environment. In simulations, the cut-off frequency of the HPF f_{cut} was designed to be 0.01 Hz. The simulation results of the grid frequency and the DC-link voltage responses under two cascading 4% step-up load changes are shown in Fig. 5.

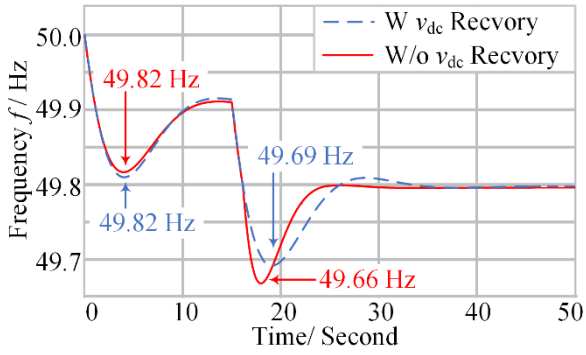

(a) Frequency f

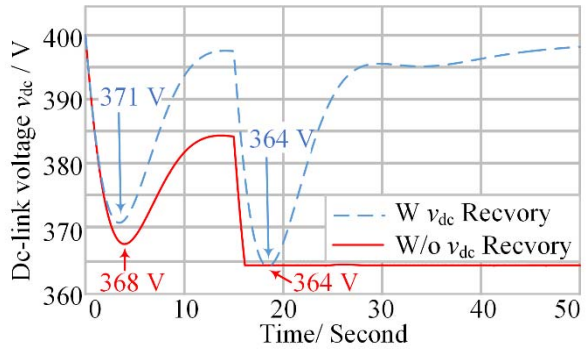

(b) DC-link capacitor voltage v_{dc}

Fig. 5. Simulation results of virtual inertia support by the GCCs with and without the DC-link voltage restoration during cascading load changes.

During the 1st load change, for the case of the conventional virtual inertia control, the maximum frequency deviation is 0.18 Hz. After the load change, the DC-link voltage can only be recovered to 384 V. During the 2nd load change, the DC-link voltage quickly reaches its low-voltage limit 364 V, and then the power converter cannot provide power to support the grid frequency, and the maximum frequency deviation is 0.34 Hz.

When the proposed virtual inertia control with the DC-link voltage restoration is activated, the maximum frequency deviation during the 1st load change is around 0.18 Hz, nearly the same as the case of the conventional virtual inertia control. After the 1st load change, the DC-link voltage can be recovered to 398 V, e.g. 99.5% of the nominal value. After that, the maximum frequency deviation during the 2nd load change is 0.31 Hz, a nearly 9% reduction as compared with the previous case can be expected.

B. Experimental results

A small-scale power system consisting of a virtual synchronous generator (VSG) and a GCC has been built in the laboratory, and a photo of the experiment platform is shown in Fig. 6. The VSG is used to emulate the synchronous generator so that the effectiveness of the proposed DC-link voltage restoration method for GCCs can be validated, and the design process of VSGs is given in [14].

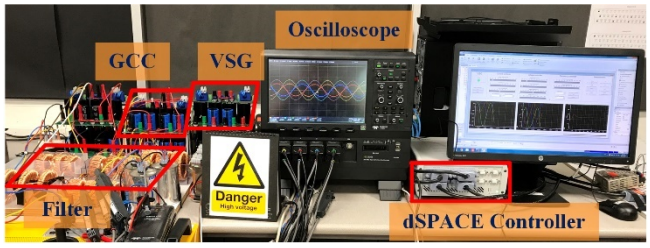

Fig. 6. Photo of the experiment platform.

In experiments, two cascading 4% step-up load changes are applied sequentially to the power system. The relevant results are shown in Fig. 7. For the case with the conventional virtual inertia control, the maximum frequency deviation is 0.18 Hz during the 1st load change. After the inertia support, the DC-link voltage only reaches 385 V, which is in proportion to the grid frequency. During the 2nd load change, the DC-link voltage quickly touches its saturation point, e.g. 364 V, and thus, the GCC cannot provide power to support the grid frequency. The maximum frequency deviation during the 2nd load change is 0.34 Hz.

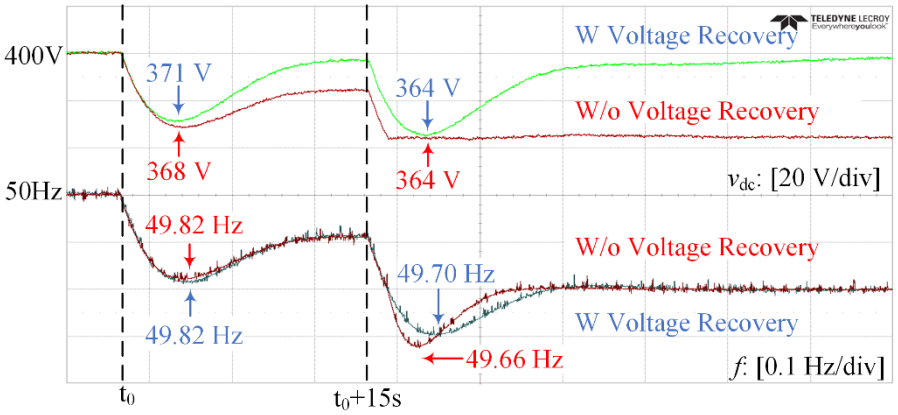

Fig. 7. Experimental results of virtual inertia support by the GCCs with and without the DC-link voltage restoration.

When the proposed virtual inertia control with the DC-link voltage restoration method is enabled, the maximum frequency deviation during the 1st load change is around 0.18 Hz, nearly the same as the case of the conventional virtual inertia control, indicating that the accuracy of inertia support is maintained. After the 1st load change, the DC-link voltage can be restored to 395 V, e.g. the 98.8% of the nominal DC-link voltage. During the 2nd load change, the maximum frequency deviation is 0.30 Hz. That is, a 11.78% reduction as compared with the case without the proposed method can be achieved. It can be concluded from the experimental results that the proposed control can quickly recover the DC-link voltage to its nominal value and allow the GCC to provide multiple inertia support for cascading frequency events.

V. Conclusion

This paper has proposed an autonomous DC-link voltage restoration method for grid-connected power converters to provide virtual inertia. The proposed method employs a high-pass filter to extract only the high-frequency components from the grid frequency for inertia emulation. The design principles of the cut-off frequency for the high-pass filter is discussed in this paper. With the proposed method, the DC-link voltage of the grid-connected power converters providing the virtual inertia can be automatically restored in quasi-steady state after releasing the power required for virtual inertia, and thus the abnormal working conditions of the power converter are avoided. Moreover, with the autonomously restored DC-link voltage, it is possible for grid-connected power converters to provide multiple grid frequency support during cascading frequency events. Simulation and experimental results have verified the feasibility and effectiveness of the proposed method.

Acknowledgement

This research is supported by the National Research Foundation, Prime Minister's Office, Singapore under the Energy Innovation Research Programme (EIRP) Energy Storage Grant Call and administrated by the Energy Market Authority (NRF2015EWT-EIRP002-007).

References

[1] Y.-K. Wu, J.-H. Lin, and H.-J. Lin, "Standards and Guidelines for Grid-Connected Photovoltaic Generation Systems: A Review and Comparison," IEEE Transactions on Industry Applications, vol. 53, no. 4, pp. 3205-3216, 2017.

[2] R. Singh and R. C. Bansal, "Review of HRESs based on storage options, system architecture and optimisation criteria and methodologies," *IET Renewable Power Generation,* vol. 12, no. 7, pp. 747-760, 2018.

[3] P. Kundur, N. J. Balu, and M. G. Lauby, *Power system stability and control*. McGraw-hill New York, 1994.

[4] A. E. M. Operator, "International Review of Frequency Control Adaptation," 2016, Available: https://www.aemo.com.au/-/media/Files/Electricity/NEM/Security_and_Reliability/Reports/2016/FPSS---International-Review-of-Frequency-Control.pdf.

[5] S. Wang, J. Hu, X. Yuan, and L. Sun, "On inertial dynamics of virtual-synchronous-controlled DFIG-based wind turbines," *IEEE Transactions on Energy Conversion,* vol. 30, no. 4, pp. 1691-1702, 2015.

[6] Y. Li, Z. Xu, and K. P. Wong, "Advanced control strategies of PMSG-based wind turbines for system inertia support," *IEEE Transactions on Power Systems,* vol. 32, no. 4, pp. 3027-3037, 2017.

[7] L. Miao, J. Wen, H. Xie, C. Yue, and W.-J. Lee, "Coordinated control strategy of wind turbine generator and energy storage equipment for frequency support," *IEEE Transactions on Industry Applications,* vol. 51, no. 4, pp. 2732-2742, 2015.

[8] F. Díaz-González, M. Hau, A. Sumper, and O. Gomis-Bellmunt, "Coordinated operation of wind turbines and flywheel storage for primary frequency control support," *International Journal of Electrical Power & Energy Systems,* vol. 68, pp. 313-326, 2015.

[9] A. F. Hoke, M. Shirazi, S. Chakraborty, E. Muljadi, and D. Maksimovic, "Rapid Active Power Control of Photovoltaic Systems for Grid Frequency Support," *IEEE Journal of Emerging and Selected Topics in Power Electronics,* vol. 5, no. 3, pp. 1154-1163, 2017.

[10] J. Fang, H. Li, Y. Tang, and F. Blaabjerg, "Distributed Power System Virtual Inertia Implemented by Grid-Connected Power Converters," *IEEE Transactions on Power Electronics,* in press.

[11] J. Machowski, J. Bialek, J. R. Bumby, and J. Bumby, *Power system dynamics and stability*. John Wiley & Sons, 1997.

[12] N. R. Subcommittee, "Balancing and Frequency Control," Princeton 2011, Available: https://www.nerc.com/docs/oc/rs/NERC%20Balancing%20and%20Frequency%20Control%20040520111.pdf.

[13] S. El Itani, U. D. Annakkage, and G. Joos, "Short-term frequency support utilizing inertial response of DFIG wind turbines," in *Power and Energy Society General Meeting, 2011 IEEE*, 2011, pp. 1-8: IEEE.

[14] J. Fang, Y. Tang, H. Li, and X. Li, "A Battery/Ultracapacitor Hybrid Energy Storage System for Implementing the Power Management of Virtual Synchronous Generators," *IEEE Transactions on Power Electronics,* vol. 33, no. 4, pp. 2820-2824, 2018.